Bottom-up creation of an artificial cell covered with the adhesive bacterionanofiber protein AtaA

Kosaku Noba,[†,#] Masahito Ishikawa,[†,#] Atsuko Uyeda, [‡] Takayoshi Watanabe,[§] Takahiro Hohsaka,[§] Shogo Yoshimoto,[†] Tomoaki Matsuura,[*,‡] and Katsutoshi Hori[*,†]

[†]Department of Biomolecular Engineering Graduate School of Engineering, Nagoya University, Furo-cho, Chikusa-ku, Nagoya 464-8603, Japan

[‡]Department of Biotechnology, Graduate School of Engineering, Osaka University 2-1 Yamadaoka, Suita, Osaka 565-0871, Japan

[§]School of Materials Science, Japan Advanced Institute of Science and Technology 1-1 Asahidai, Nomi, Ishikawa 923-1292, Japan

Author Contributions

[#]K.N. and M.I. contributed equally to this work.

*Corresponding Authors

(K.H.) E-mail: khori@chembio.nagoya-u.ac.jp

(T.M.) E-mail: matsuura_tomoaki@bio.eng.osaka-u.ac.jp

Abstract

The bacterial cell surface structure has important roles for various cellular functions. However, research on reconstituting bacterial cell surface structures are limited. This study aimed to bottom-up create a cell-sized liposome covered with AtaA, the adhesive bacterionanofiber protein localized on the cell surface of *Acinetobacter* sp. Tol 5, without the use of the protein secretion and assembly machineries. Liposomes containing a benzylguanine derivative–modified phospholipid were decorated with a truncated AtaA protein fused to a SNAP-tag expressed in a soluble fraction in *Escherichia coli*. The obtained liposome showed a similar surface structure and function to that of native Tol 5 cells and adhered to both hydrophobic and hydrophilic solid surfaces. Furthermore, this artificial cell was able to drive an enzymatic reaction in the adhesive state. The developed artificial cellular system will allow for analysis of not only AtaA, but also other cell surface proteins under a cell-mimicking environment. In addition, AtaA-decorated artificial cells may inspire the development of biotechnological applications that require immobilization of cells onto a variety of solid surfaces.

Introduction

An artificial cell is a cell-like compartment that harbors various compounds and biological systems, thereby mimicking part of the cellular functions. Bottom-up creation of an artificial cell has been regarded as one of the approaches to understand the cellular functions that are too complex to interpret in conventional "top-down" studies[1]. Mimicking the cellular functions with defined molecules enables us to remove the complexity from a system, making it easier to interpret the dynamics or the behavior induced by the molecules. Furthermore, bottom-up creation of an artificial cell occasionally provides unexpected results that lead to new insights into biology and inspires researchers to develop new technologies[2, 3]. To date, the liposome has been one of the most popular and cell-mimicking compartments used to create artificial cells.

Cellular functions such as uptake of substrates[4, 5], protein translocation[6], phospholipid biosynthesis[7], cell division and related processes[8, 9], membrane protein evolution[10, 11], and cascade reaction by a genetic circuit[12-14] have been introduced into liposomes. Unlike liposomes, the surface of a living cell is structurally complex due to the presence of various proteins, including integral and peripheral membrane proteins, as well as cell appendages. These structures play important roles for cellular functions such as ligand recognition, cell-cell communication, motility, and adhesion. Nevertheless, bottom-up creation of an artificial cell that mimics bacterial cell surface structures is limited.

More than 90% of environmental bacteria live in an adhesive state rather than a planktonic state[15, 16]; thus, adhesion to a solid surface is critical for the lifestyle of bacteria. Bacterial adhesion to solid surfaces has also an advantage in wide range of bioprocesses, most of which are conducted by enzymes, including bioproduction, bioremediation, and wastewater treatment, as adherent bacteria can be immobilized even under flow conditions, and can enhance their capability through high-density accumulation of cells[17]. Adhesion to a solid surface is achieved by various molecules, including exopolymeric substances produced by bacteria, or via the presence of cell surface appendages[17]. However, artificial cells harboring enzymes that adhere to solid surfaces by mimicking the bacterial cell surface have not yet been created. One of the reasons for this is the difficulty in synthesizing proteins on the bacterial cell surface, which mostly contains transmembrane or membrane interacting domains. In addition, natural bacterial cells use transport machinery to secrete and assemble proteins on the cell surface[18, 19]. Although there has been some partial success [6, 20], full reconstitution of such complex molecular machinery in artificial cells is yet to be achieved.

Trimeric autotransporter adhesin (TAA) is a cell appendage that mediates adhesion of Gram-negative bacteria to solid surfaces[21]. TAA forms fibers on the order of ten to hundreds of nanometers in length, composed of three polypeptides encoded by a single gene, *i.e.*, a homotrimer. AtaA, a TAA discovered in a sticky Gram-negative bacterium,

Acinetobacter sp. Tol 5, forms peritrichate nanofibers ≈225 nm in length and 4 nm in thickness on the cell surface[22]. Most of the TAAs reported to date exhibit specific adhesiveness to biotic surfaces such as extracellular matrix proteins on host tissues, whereas AtaA nonspecifically adheres to abiotic surfaces made of various materials, such as hydrophobic plastics, hydrophilic glasses, and metals. Furthermore, the adhesiveness mediated by AtaA is much higher than that mediated by YadA, which is the most well-studied TAA. Due to this adhesive feature of AtaA, bacteria covered with AtaA fibers can be immobilized on the surface of various materials[23, 24].

In this study, we aimed to create cell-sized liposomes covered with the adhesive nanofiber protein AtaA, thereby creating an artificial cell that adheres to various solid surfaces and can perform a reaction catalyzed by an encapsulated enzyme (Figure 1). Our strategy for the construction of surface-decorated artificial cells without the use of complex transport machinery allows for characterization and functional analyses of not only AtaA, but also other peripheral membrane proteins and cell appendages under cell-mimicking environments in the absence of other cell surface components.

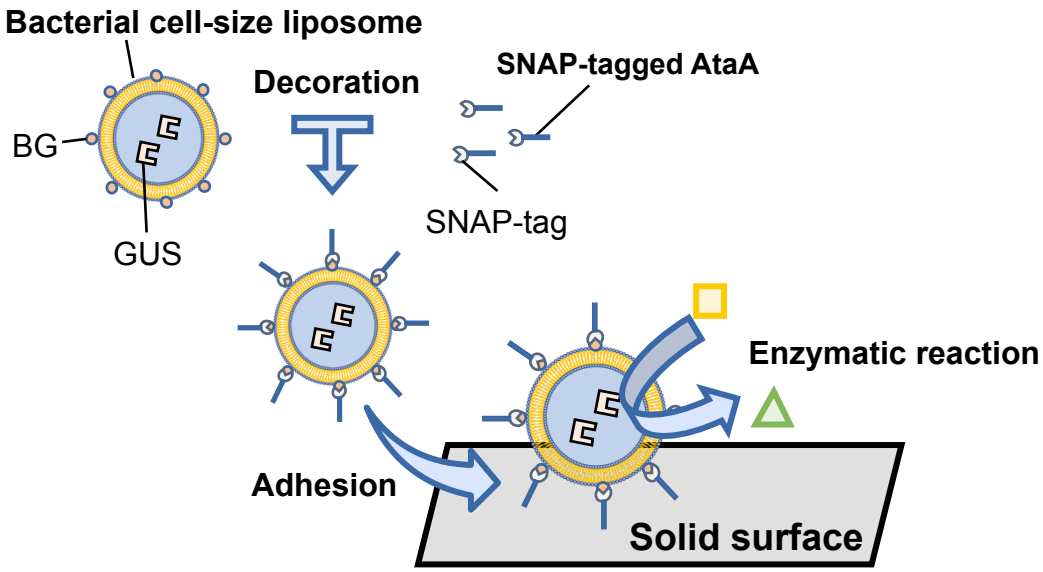

Figure 1. Illustration of the concept presented in this study. A bacterial cell-size liposome

was decorated with the adhesive nanofiber protein AtaA by the interaction between a SNAP-tag fused with the AtaA and benzylguanine (BG)-group on the liposome. Since β-glucuronidase (GUS) is encapsulated within the liposome, the enzymatic reaction occurs on a solid surface.

Results

Decorating cell-sized liposomes with AtaA

Natural bacterial cells use transport machinery to secrete and assemble huge cell appendages on the cell surface[18, 19]. Full reconstitution of such complex molecular machinery in artificial cells is yet to be achieved. To cover artificial cells with AtaA, we combined chemical synthesis and protein engineering; i.e., we used the chemical reaction between a benzylguanine (BG) derivative–modified phospholipid and AtaA fused to the SNAP-tag (Figure 1). The SNAP-tag is a 20-kDa protein that forms a covalent bond with a BG derivative[25, 26]. First, we designed and constructed a plasmid for the expression of a fusion protein of an AtaA fragment and the SNAP-tag in *Escherichia coli*. Membrane proteins and proteins with high molecular weights (> 60 kDa) are generally difficult to express in *E. coli*[27]. Hence, we assumed it difficult to express the full-length of AtaA in *E. coli,* because AtaA is a huge protein whose molecular weight is over 350 kDa and its C-terminal trans-membrane (TM) domain was embedded in the outer membrane. To decrease the molecular weight of AtaA while retaining its function and to enable its expression in the cytoplasm of *E. coli*, we deleted its signal peptide ($AtaA_{1\text{-}58}$), Chead, Cstalk, and TM domains ($AtaA_{2904–3630}$), which are not essential for its adhesive function[28], yielding a truncated AtaA, NheadNstalk (NhNs)-AtaA (280 kDa) (Figure 2a). Because the GCN4 adaptor[29] assists in the trimerization of recombinant AtaA fragments[28], the GCN4 adaptor sequence was connected to the leucine residue at the C-terminus of NhNs-AtaA, followed by the SNAP-tag and Strep-tag (8 amino acids). Because the

NhNs-AtaA peptide trimerizes and the SNAP-tag is a monomer protein, the resulting chimera polypeptide should form a fusion protein of a trimer of truncated AtaA and three SNAP-tag molecules. This fusion protein was designated as NhNs-AtaA-SNAP. When NhNs-AtaA-SNAP was expressed in *E. coli*, more than half of the protein appeared in the soluble fraction, suggesting that a significant fraction of the expressed protein was folded properly (Figure S1). This is one of the largest fusion proteins that forms a complex quaternary structure (≈1 MDa when forming trimers) that is synthesized as a recombinant protein in the cytoplasm of *E. coli*.

The bacterial cell size-liposomes (on average about 0.8 μm in diameter) were prepared by mixing BG-modified 1,2-distearoyl-*sn*-glycero-3-phosphoethanolamine (DSPE)[30] and Egg yolk phosphatidylcholine (Egg-PC) denoted as BG-liposome or using only Egg-PC denoted as EggPC-liposome as a control. For liposome decoration with NhNs-AtaA-SNAP, these liposomes were mixed with the supernatant of a cell lysate from *E. coli* BL21 (DE3) harboring a plasmid encoding NhNs-AtaA-SNAP (pNhNs-SNAP), denoted as BL21 (pNhNs-SNAP). Because these liposomes can be harvested by centrifugation, the decorated liposome should be obtained as precipitants. To confirm liposome decoration with NhNs-AtaA-SNAP, the precipitants were subjected to SDS-PAGE and subsequent immunodetection using anti-AtaA antiserum and anti-SNAP antibody. Signals were detected by both antibodies when BG-liposome was mixed with the supernatant of the cell lysate of BL21 (pNhNs-SNAP), but not when EggPC-liposome was mixed with the same lysate (Figure 2b). No signal was detected when BG- and Egg-PC liposomes were mixed with the supernatant of a cell lysate from *E. coli* BL21 (DE3), denoted as BL21 (WT). This result suggests that the SNAP-tag fused to a huge complex of truncated AtaA was functional.

The liposome with NhNs-AtaA was further analyzed using fluorescence cytometry (FCM). All liposomes containing fluorescence dye Alexa Fluor 647 (AF647) in their aqueous phase for detection purposes were immunostained with anti-AtaA antiserum

followed by an anti-rabbit IgG antibody conjugated to Alexa Fluor 488 (AF488). As shown in Figure 2c, the two-dimensional plot displayed the fluorescence signals of both AF488 and AF647 when BG-liposomes were treated with the cell lysate of BL21 (pNhNs-SNAP), whereas only the fluorescence signal of AF647 was detected from other liposomes. The results of the immunodetection and FCM analysis suggest that liposomes were decorated by NhNs-AtaA-SNAP via the covalent bond between the SNAP-tag and the BG-group.

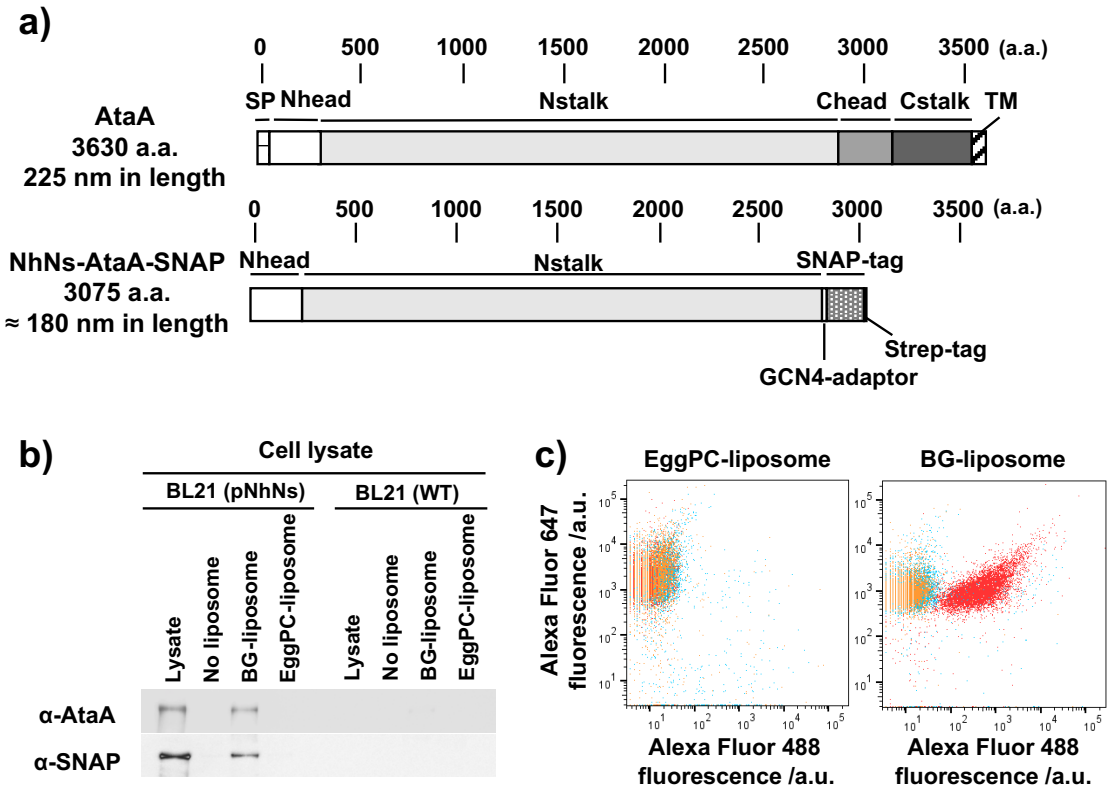

Figure 2. Decoration of a liposome with a truncated AtaA recombinant protein. a) Schematics of the native AtaA and NhNs-AtaA-SNAP. SP, signal peptide; TM, transmembrane domain. b) Immunodetection of NhNs-AtaA-SNAP associated with the liposomes. BG-liposome and EggPC-liposome were treated either with the supernatant of the cell lysate from BL21 (pNhNs-SNAP) or BL21 (WT). Precipitated liposomes were subjected to immunodetection using anti-AtaA antiserum or anti-SNAP-tag antibody as

the primary antibody. c) Fluorescence cytometry (FCM) analysis of liposomes. The liposomes treated with the cell lysates were immunostained with anti-AtaA antiserum and anti-rabbit IgG conjugated to AF488. AF647 was encapsulated inside both liposomes. Orange, blue, and red dots represent liposomes treated with 10 mM Tris-HCl buffer (pH 9.0), the supernatant of the cell lysate from BL21 (WT), and the cell lysate from BL21 (pNhNs-SNAP), respectively.

AtaA on the liposome forms the nanofiber

To investigate whether NhNs-AtaA forms a nanofiber structure on the liposome, the size distribution of the decorated liposome was analyzed by dynamic light scattering (DLS). In the case of bacterial cells (Tol 5 and its Δ*ataA* mutant), the size distribution by DLS analyses displayed a clear difference between the presence and absence of AtaA fibers (Figure 3a). Note that DLS analyses were performed under a condition where AtaA exhibit less adhesive activity (see Methods). The dominant size of Tol 5 cells was about 440 nm larger than that of Δ*ataA* cells; this difference nearly corresponds to the size predicted from the length of native AtaA (225 nm × 2)[31]. Since the length of the NhNs-AtaA fiber was deduced to be about 180 nm, the size of the decorated liposome should be larger than a non-decorated one. In non-decorated BG- and EggPC-liposomes, their peak of the size distribution was 825 nm in diameter (Figure S2a). When a BG-liposome was treated with the cell lysate from BL21 (pNhNs-SNAP), the peak at 825 nm shifted to 1281 nm (Figure 3b); this difference nearly corresponds to the size predicted from the length of NhNs-AtaA (180 nm × 2). The peak shift did not occur when an EggPC-liposome was treated with the cell lysate containing NhNs-AtaA-SNAP (Figure S2b). Furthermore, we attempted to directly observe the surface of the BG-liposome decorated with NhNs-AtaA-SNAP. Based on previous observations of Tol 5 cells using transmission electron microscopy (TEM), the NhNs-AtaA part of the fusion protein should be visible as a nanofiber on the BG-liposome[22, 32].. As expected, many fibrous structures were

observed on the surface of BG-liposomes treated with the cell lysate containing NhNs-AtaA-SNAP, whereas no fibers were visible on non-decorated BG-liposomes (Figure 3c). The DLS results and TEM image provided evidence for the decoration of the BG-liposome with NhNs-AtaA fibers, and demonstrated that we successfully created an artificial cell partially mimicking the bacterial cell surface structure without the use of membrane translocation machinery. In addition, the features of the observed nanofiber, which strongly resembles those of Tol 5 cells[22, 32], strongly suggests the formation of a trimer of NhNs-AtaA with adhesive function.

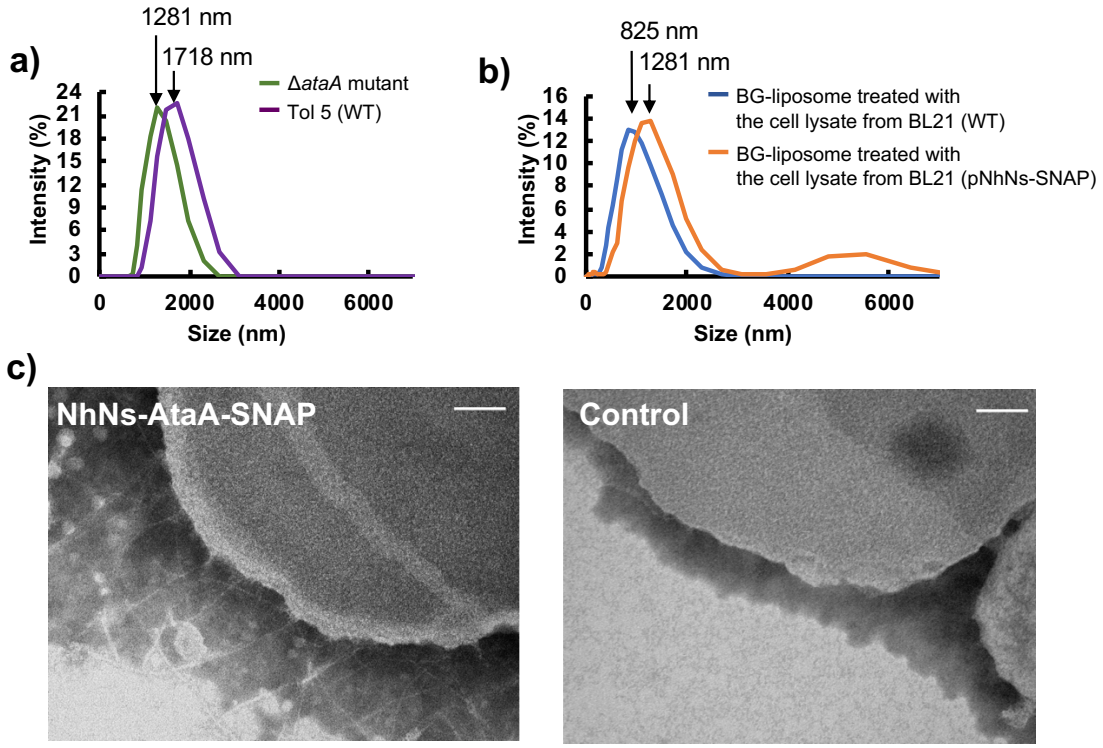

Figure 3. Decorating liposomes with truncated AtaA fiber. a) Size distributions of bacterial cells of *Acinetobacter* sp. Tol 5 and its *ataA*-deficient mutant, measured by DLS. b) The size distribution of BG-liposomes treated with the cell lysate from BL21 (WT) and BL21 (pNhNs-SNAP) measured by DLS. (c) TEM images of BG-liposomes treated with the cell lysate from BL21 (pNhNs-SNAP) (NhNs-AtaA-SNAP) and with the cell lysate from BL21 (WT) (Control). Scale bars indicate 50 nm.

Artificial cells exhibit adhesive functions

To determine whether NhNs-AtaA fibers on BG-liposomes have an adhesive function, we subjected liposomes to the adherence assay using two 96-well plates with different physicochemical properties: one consisting of hydrophobic polystyrene (PS), and the other of hydrophilic glass; native AtaA fiber adheres to both of these surfaces[22]. Since all liposomes contained AF647 in their aqueous phase, the liposomes adhering to the surface could be evaluated by their fluorescence. To efficiently contact the liposomes, whose densities were close to that of water, with the bottom surfaces, the plates were weakly centrifuged, and then unbound (non-adhesive) liposomes were washed out. As a result, significant fluorescence signals were detected from both PS and glass-bottom plates with decorated BG-liposomes, and their fluorescence intensities increased with increasing protein concentration of cell lysate used for preparation of decorated BG-liposomes (Figure 4ab). Conversely, the increase in fluorescence intensity was not detected when EggPC-liposome was treated with the same cell lysate.

To further confirm that the increase in fluorescence intensity could be attributed to the adhesive function of NhNs-AtaA, we inhibited the decoration of BG-liposome with NhNs-AtaA-SNAP in two different ways: one was the blocking of BG-groups on a liposome using SNAP-tagged GFP; the other was the inactivation of the SNAP-tag fused with NhNs-AtaA using SNAP-Surface Block, a compound that reacts with the SNAP-tag. Both of the inhibition treatments significantly decreased the fluorescence intensity on the plate surface (Figure S3). These results indicate that NhNs-AtaA-SNAP is coupled to the BG-liposome via the BG and SNAP-tag interaction and the NhNs-AtaA fiber exhibits adhesive features similar to those of native AtaA fiber. NhNs-AtaA-SNAP retained the functions of both AtaA and SNAP-tag.

Finally, we examined if the constructed artificial cell can drive an enzymatic reaction inside a liposome adhering to the plate surface. As a model enzyme, β-glucuronidase

(GUS) was encapsulated in BG- and EggPC-liposomes. These liposomes were treated with the supernatant of the cell lysate containing NhNs-AtaA-SNAP, placed into wells of the PS plates, and immobilized on plate surfaces following the adherence assay procedure described above. We then added TokyoGreen-βGlu[5], a membrane-permeable substrate for GUS, which emits fluorescence only after hydrolysis to monitor the enzymatic reaction. A significant increase in fluorescence intensity was detected only from wells on which NhNs-AtaA-SNAP–decorated liposomes were immobilized (Figure 4c). This result indicates that GUS encapsulated in a liposome is active inside the decorated liposome immobilized on the plate surface.

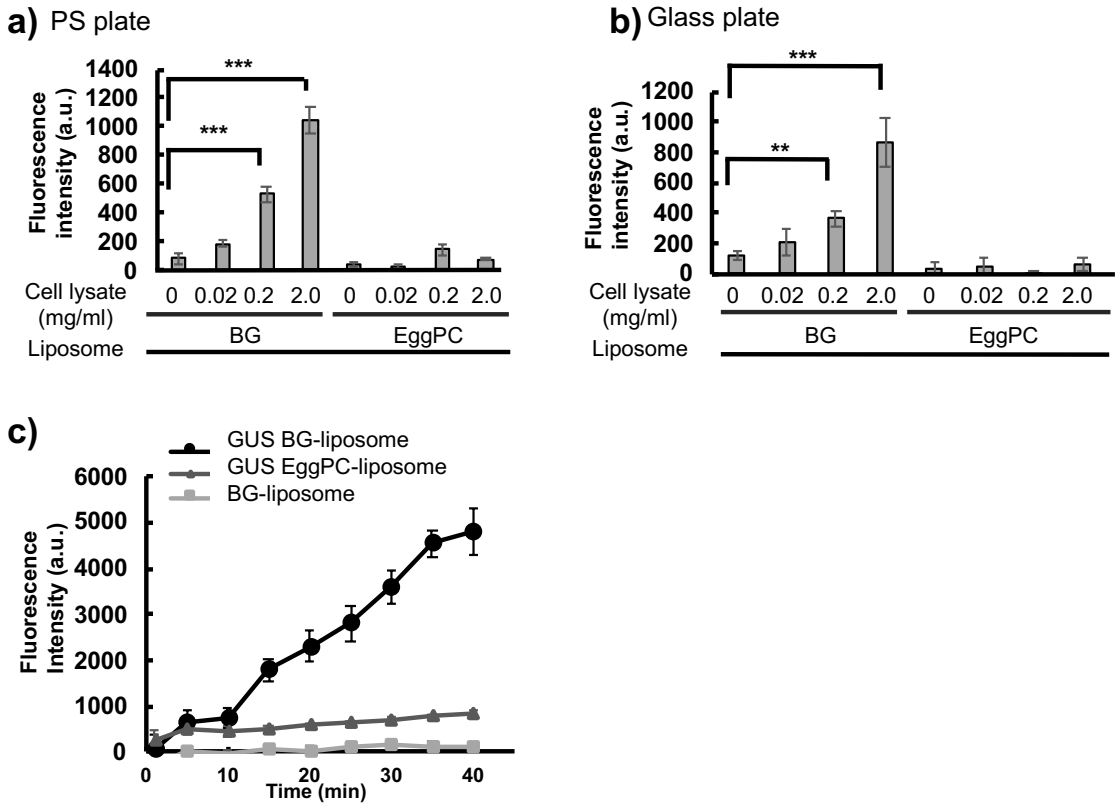

Figure 4. Adherence assay of liposomes using a) polystyrene and b) glass-bottom plates. BG- and EggPC-liposomes were treated with supernatant of the cell lysate from BL21 (pNhNs-SNAP) at different concentrations. Adhering liposomes were detected by the

fluorescence of AF647 encapsulated inside the liposome. Data are expressed as mean ± SEM (n=6). Statistical analysis was performed by Welch's t test. Statistical significance: **P<0.01, ***P<0.001. (c) Time course of the hydrolysis of TokyoGreen-βGlu by GUS encapsulated in liposomes immobilized on the plate surface. The encapsulating BG- and EggPC-liposomes (GUS BG-liposome and GUS EggPC-liposome, respectively) were treated with supernatant of the lysate containing NhNs-AtaA-SNAP. As a negative control for the enzymatic reaction, BG-liposome without GUS (BG-liposome) was used. Data are expressed as mean ± SEM (n=3).

Discussion

This study aimed to create, using a bottom-up approach, an artificial bacterial cell capable of adhering to solid surfaces. This was accomplished by assembling BG-modified cell-size liposomes and a truncated AtaA-SNAP fusion protein that exists in complexes as large as 1 M Da (trimer of 305 kDa). We did not use the protein secretion machinery (translocon)[18] or β-barrel–assembly machinery (BAM) complex[19] involved in the formation of appendages like AtaA in natural cells. The TEM image of the NhNs-AtaA-SNAP-decorated liposome shown in Figure 3c bears a striking resemblance to TEM images of Tol 5[22, 32]. This is the first study to create a bacterial mimic of a cell surface structure from defined materials.

One strategy for characterizing the extracellular part of a cell surface protein of interest is to investigate it directly at the cellular level. Although this strategy is useful, many other proteins are present on the cell surface, and their effects on the properties of the protein of interest are difficult to eliminate. *In vitro* analyses using a purified protein produced by its original strain or recombinant strains, typically after removing the transmembrane domain, is an alternative approach to characterizing the extracellular part of the cell surface protein of interest. Although this method gives useful information about molecular characteristics of the protein of interest, the actual functions and characteristics

of the protein on the cell surface are difficult to realize due to uncontrolled orientation, direction, and localization. In this study, we synthesized a truncated AtaA recombinant protein without the signal peptide or transmembrane domain in the cytosol of *E. coli*, and succeeded in immobilizing it on the liposome surface by simply mixing the supernatant of an *E. coli* cell lysate with BG liposomes. Unlike isolated protein, the orientation of the recombinant protein fiber assembled on the liposome surface mimics its intact condition on the cell surface and its function on bacterial cells. As long as the extracellular part of cell surface proteins can be synthesized in the cytosol of an *E. coli* or other cells, this strategy should be applicable to other cell surface proteins for their characterization and functional analyses on the artificial cell membrane in the absence of other surface proteins.

In the DLS analysis of the NhNs-AtaA–decorated liposome, a small peak was observed between 4000 and 6500 nm, which might correspond to a small fraction of liposome cluster. Native AtaA mediates autoagglutination as well as adhesion to solid surfaces, but these adhesive functions are lost in the condition of low ionic strength[33]. When preparing the sample for DLS analysis, Tol 5 cells were suspended in pure water to prevent the formation of cell aggregates. Conversely, a liposome decorated with NhNs-AtaA-SNAP was analyzed by DLS in 10 mM Tris-HCl buffer, a condition where cell aggregates are formed when using Tol 5 cells. However, the intensity of the peak observed on the decorated liposome was weak and the cluster size was small; under the same condition, the cell aggregates of Tol 5 were too large to be analyzed by DLS (data not shown). Therefore, the ability of NhNs-AtaA on the liposome to cause autoagglutination is thought to be quite low compared with native AtaA on Tol 5 cells. Although the mechanism of the difference between NhNs-AtaA and native AtaA remain unclear, the adhesive nature without autoagglutination of NhNs-AtaA might be convenient for the biotechnological application of functional liposomes.

A mammalian cell specifically adheres to other cells and the extracellular matrix (ECM), namely, biotic solid surfaces via cell surface proteins such as cadherin and

296 integrin. Artificial cells mimicking a mammalian cell surface were constructed by adding
297 integrin to the liposome surface[34-36]. These artificial cells exhibited adhesion to ECM-
298 coated solid surfaces. In addition to specific adhesion to biotic surfaces, bacterial cells
299 nonspecifically adhere to abiotic surfaces via the presence of cell appendages[17]. In
300 particular, AtaA exhibits remarkably high adhesiveness, thereby immobilizing bacterial
301 cells onto various solid surfaces[22-24]. Unlike artificial cells mimicking the mammalian cell
302 surface, those mimicking the bacterial cell surface can adhere to both hydrophobic and
303 hydrophilic surfaces via NhNs-AtaA without ECM-coating of the solid surfaces. This
304 feature should be beneficial for biotechnological applications that require immobilization
305 of an artificial cellular system onto a variety of solid surfaces.

306 Living cells (often modified genetically) immobilized onto solid supports have been
307 used as whole cell catalysts for bioproduction, bioremediation, and wastewater
308 treatment[17], despite the risk of release of genetically modified organisms into the
309 environment. These artificial cells may be used as an alternative in these processes.
310 Artificial cells have the advantage that all of their extracellular and intracellular
311 components are designed. In this study, we encapsulated GUS inside the artificial cell and
312 employed the membrane-permeable substrate as a model system. GUS can be substituted
313 with other enzymes including those that are difficult to handle with living cells such as
314 membrane-associated enzymes and/or enzymes that exhibit cell toxicity. Membrane-
315 impermeable substrates can also be used by forming nanopores on an artificial cell
316 membrane, for example with α-hemolysin[4]. Therefore, artificial cells may be useful for
317 developing new biotechnological applications encapsulating various chemical reaction
318 systems, mimicking whole-cell catalysts. Unlike living cells, artificial cells do not
319 replicate, but can still catalyze reactions of interest on a solid surface. These properties of
320 artificial cells may be attractive in environments where the use of genetically modified
321 organisms is prohibited.

322 Although the artificial cell constructed in this study was robust enough to endure

mixing with cell lysates, immobilizing to solid surfaces, and performing an enzyme reaction, further stabilization by introducing an artificial cytoskeleton, for example by incorporating DNA origami technology[37], may give versatile catalytic activity under a wide range of conditions.

In summary, using a bottom-up approach, we succeeded in constructing an enzyme-encapsulating artificial cell that adhered to solid surfaces. This artificial cellular system is expected to reveal the properties of cell surface proteins without interference from other cell surface components, and to inspire the development of new biotechnological applications that require cell immobilization onto a variety of solid surfaces.

Methods

Construction of plasmids

The primers used in this study are listed in Table S1. A DNA fragment encoding $AtaA_{59\text{-}325}$ was amplified from pDONR::*ataA*[22] by a PCR using the primer set AtaA59F/AtaA325R, digested with XbaI and BsaI, and ligated into the same site of pIBA-GCN4tri-His[29], generating pIBA-$AtaA_{59\text{-}325}$-GCN4tri-His. Subsequently, a DNA fragment encoding SNAP-tag was amplified from $pSNAP_f$ Vector (New England Biolabs Inc, Ipswich, MA) by a PCR using the primer set SNAPF/SNAPR. By using an In-Fusion HD Cloning Kit (Takara Bio, Shiga, Japan), this amplicon was fused to a DNA fragment amplified from pIBA-$AtaA_{59\text{-}325}$-GCN4tri-His by an inverse PCR using the primer set HisF/GCN4R, generating pIBA-$AtaA_{59\text{-}325}$-SNAP-His. To add a BglII site for further cloning, a DNA fragment was amplified from pIBA-$AtaA_{59\text{-}325}$-SNAP-His by an inverse PCR using the primer set iPCR-BglII-F/iPCR-BglII-R and then self-ligated, generating pIBA-$AtaA_{59\text{-}325}$-BglII-SNAP-His. To substitute the C-terminal His-tag with Strep-tag, a DNA fragment was amplified from pIBA-$AtaA_{59\text{-}325}$-BglII-SNAP-His by an inverse PCR using the primer set iPCR-Strep-F/iPCR-Strep-R and then self-ligated, generating pIBA-$AtaA_{59\text{-}325}$-BglII-SNAP-Strep. To delete the initial methionine residue in the GCN4

adaptor, two DNA fragments were amplified from pIBA-AtaA$_{59\text{-}325}$-BglII-SNAP-His and pIBA-AtaA$_{59\text{-}325}$-BglII-SNAP-Strep by an inverse PCR using the primer set iPCR-Met-F/iPCR-Met-R, and then self-ligated, generating pIBA-AtaA$_{59\text{-}325}$-BglII-SNAP-His-ΔMet and pIBA-AtaA$_{59\text{-}325}$-BglII-SNAP-Strep-ΔMet, respectively. pDONR::*ataA* was digested with BspT104I and BglII, and the resultant DNA fragment was ligated into the same site of pIBA-AtaA$_{59\text{-}325}$-BglII-SNAP-His-ΔMet, generating pIBA-NhNs-SNAP-His. Finally, pIBA-AtaA$_{59\text{-}325}$-BglII-SNAP-Strep-ΔMet was digested with BglII and NheI, and the resultant DNA fragment was ligated into the same site of pIBA-NhNs-SNAP-His, generating pNhNs-SNAP.

Bacterial strains and culture conditions

E. coli BL21 (DE3) and its transformant harboring the pNhNs-SNAP plasmid were grown at 37°C in Luria-Bertani (LB) medium. *Acinetobacter* sp. Tol 5 and its Δ*ataA* mutant were grown at 28°C in LB medium. Ampicillin (100 μg/mL) was added for the *E. coli* transformant. For the production of the NhNs-AtaA-SNAP recombinant protein, *E. coli* transformant cells were grown to an optical density at 600 nm (OD_{600}) = 0.5–0.7, and thereafter, 0.20 μg/mL anhydrotetracycline was added. After incubation at 18°C for 16 h, cells were harvested, resuspended in a buffer (25 mM Tris-HCl, 20 mM imidazole, 150 mM NaCl, pH 9.0), lysed by sonication, and centrifuged at 10,000 *g* for 10 min. To confirm production of NhNs-AtaA-SNAP in the *E. coli* strain, supernatant and pellet fractions were subjected to SDS-PAGE analysis.

SDS-PAGE and immunodetection

To examine the decoration of liposomes with NhNs-AtaA-SNAP, liposome suspensions were mixed with the same volume of SDS-sample buffer [0.125 M Tris-HCl buffer (pH 6.8), 4% (wt/vol) SDS, 10% (wt/vol) sucrose, 0.01% (wt/vol) bromophenol blue, 10% (wt/vol) 2-mercaptoethanol], heated at 100°C for 5 min, and subjected to SDS-

PAGE. For immunodetection, the proteins were transferred to a PVDF membrane with a constant current of 100 mA for 90 min. The blotted membrane was blocked for 1 h at room temperature with a 5% (wt/vol) skim milk solution, and treated for 1 h at room temperature with anti-AtaA$_{699\text{-}1014}$ antiserum[22] or anti-SNAP antibody (Medical & Biological Laboratories Co., Ltd, Nagoya, Japan) at a dilution of 1:10,000 or 1:2,000 in phosphate-buffered saline (PBS) containing 0.05% (vol/vol) Tween 20 (Calbiochem) (PBS-T), respectively. NhNs-AtaA-SNAP on the membrane was detected with a horseradish peroxidase–conjugated anti-rabbit IgG antibody (GE Healthcare) at a dilution of 1:10,000 in PBS-T, and visualized using EzWestLumi plus (ATTO).

Preparation of liposomes

Three hundred microliters of 50 mg/mL egg phosphatidylcholine (COATSOME NC-50 (EPC)) (Yuka-Sangyo Co., Ltd., Tokyo, Japan) dissolved in chloroform was rotated under vacuum in a round-bottom flask for 1 h. The lipid film was hydrated with buffer A (10 mM HEPES, pH 7.6, 50 mM potassium glutamate) supplemented with 25 μM Alexa Fluor 647, or buffer B (10 mM Tris-HCl [pH 9.0]) to obtain 300 μL of 50 mg/mL lipid solution. For the samples with GUS, 2 μM GUS was added to buffer A. GUS was produced and purified as described previously[41]. For the samples for electron microscopy observation, 1 mg/mL BSA was added to buffer B. The lipid solution was sonicated for 10 min and vortexed for 10 s. The lipid solution was further subjected to five rounds of freeze-thaw cycles. The liposome suspension was then extruded with a mini-extruder (Avanti Polar Lipids, Alabaster, AL, USA) using a 0.8 μm VCTP isopore membrane filter at room temperature. The prepared large unilamellar vesicle (LUV) was washed by adding 1,200 μL of buffer A or buffer B to 300 μL LUV solution prepared with buffer A or B, respectively; centrifuging at 20,000 *g* for 30 min; and replacing the supernatant with 1,200 μL of fresh buffer A or B. This washing step was repeated four times.

BG-liposomes were prepared as follows. First, 14 μL of 2 mM BG-DSPE[30] dissolved

in chloroform was rotated under vacuum in a glass micro test tube for 15 min, hydrated with buffer A or buffer B. This BG-DSPE solution was then added to a final concentration of 93 μM to the LUV solution and incubated at room temperature for 20 h followed by the four-times washing steps described above.

Decoration of liposome with NhNs-AtaA-SNAP

BG- and EggPC-liposome suspensions were mixed with 2.0 mg/mL of cell lysate extracted from either *E. coli* BL21 (DE3) or its transformant harboring the pNhNs-SNAP plasmid. After 1 h of incubation at 4°C on a rotary mixer, the liposome particles were precipitated by centrifugation at 15,000 *g* for 10 min to remove unbound NhNs-AtaA-SNAP and other proteins. The precipitated liposome particles were washed twice with 10 mM Tris-HCl (pH 9.0) buffer and resuspended in the same buffer. When inhibiting the decoration of NhNs-AtaA-SNAP to the liposome, BG-liposome suspension was incubated with a purified SNAP-GFP at a final concentration of 20 μM, or 2.0 mg/mL of the cell lysate containing NhNs-AtaA-SNAP was incubated with SNAP-Surface Block (New England BioLabs Japan Inc., Tokyo, Japan) at a final concentration of 1–100 μM in 100 μL of 10 mM Tris-HCl buffer (pH 9.0) for 1 h at 4°C by inversion mixing.

Measurement of dynamic light scattering

The size of a liposome or bacterial cell was measured by dynamic light scattering using Zetasizer Nano ZSP (Malvern Instruments, UK) equipped with a He-Ne laser (wavelength, 633 nm). Liposome suspensions were diluted to 50-fold in 10 mM Tris-HCl buffer (pH 9.0) for DLS measurement. Cells of Tol 5 and Δ*ataA* mutant were harvested by centrifugation at 8,000 *g*, resuspended in deionized water, and adjusted to an OD_{660} = 0.05 with deionized water. Quartz cuvettes were filled with the samples and all the experiments were thermostatically controlled at 25°C. All the DLS measurements were made with a scattering angle of 173°. The results were given as diameters and the

431 percentages correspond to intensity values.

432

433 **Fluorescence cytometry**

434 For fluorescence cytometry analysis, the liposome suspension was diluted 100-fold in
435 10 mM Tris-HCl buffer (pH 9.0). Liposomes were treated with anti-AtaA$_{699\text{-}1014}$
436 antiserum[22] at a 1:10,000 dilution in 10 mM Tris-HCl (pH 9.0) buffer for 1 h at room
437 temperature. After the incubation, the liposomes were washed twice with 10 mM Tris-
438 HCl (pH 9.0) buffer and then treated with AF488 conjugated to anti-rabbit antibody (Cell
439 Signaling Technology, Danvers, MA, USA) at 1:1,000 dilution in 10 mM Tris-HCl (pH
440 9.0) buffer for 1 h at room temperature. After the incubation, liposomes were washed
441 twice with 10 mM Tris-HCl (pH 9.0) buffer and resuspended in the same buffer. The
442 fluorescent signals from the immunostained liposomes were measured with FACS Canto
443 II (BD Biosciences, Franklin Lakes, NJ, USA). FlowJo software (Tomy Digital Biology,
444 Tokyo, Japan) was used to create 2D plots and to compare the fluorescence intensities
445 among the samples.

446

447 **Electron microscopy**

448 The liposome suspension was diluted 50-fold in 10 mM Tris-HCl buffer (pH 9.0). The
449 liposomes were adsorbed to carbon-coated copper grids (400 mesh) and were stained with
450 2% phosphotungstic acid solution (pH 7.0) for 10 s. Subsequently, the grids were
451 performed with vacuum drying for 10 min. Grids were observed under a TEM (JEM-
452 1400 plus; JEOL Ltd., Tokyo, Japan) at an acceleration voltage of 100 kV. Digital images
453 (3296×2472 pixels) were taken with a CCD camera (EM-14830RUBY2; JEOL Ltd.,
454 Tokyo, Japan).

455

456 **Adherence and enzymatic assay**

457 Forty-five microliters of liposome suspension was placed into a 96-well polystyrene

(PS) plate (Becton, Dickinson and Company, NJ, USA) or a 96-well glass-bottom plate (Matsunami Glass Ind., Ltd, Osaka, Japan) and mixed with 5 μL of 10× phosphate-buffered saline (1.37 M NaCl, 27 mM KCl, 81mM $Na_2HPO_4 \cdot 7H_2O$, 14.7 mM KH_2PO_4) at each well. To bring liposome particles into contact with the plate surface, the plate containing liposome suspensions was centrifuged at 700 *g* at room temperature for 30 min, and the supernatant was removed. To remove unbound liposomes, wells were washed four times with a buffer (9.0 mM Tris-HCl (pH 9.0), 137 mM NaCl, 2.7 mM KCl, 8.1 mM $Na_2HPO_4 \cdot 7H_2O$, 1.47 mM KH_2PO_4) and resuspended in 50 μL of 10 mM Tris-HCl buffer (pH 9.0). The adherence of liposome was evaluated by measuring the fluorescent signal of AF647 that was encapsulated in a liposome using a micro plate reader (ARVO X3; PerkinElmer, MA, USA). The fluorescent signal was quantified using the top reading mode for a better signal-to-noise ratio. When detecting the AF647 fluorescence from liposomes adhering to the 96-well glass-bottom plate, its bottom was masked by a black plastic tape.

For the enzymatic assay by GUS encapsulated in a liposome adhering to the plate surface, liposome suspension was diluted 50-fold in 10 mM Tris-HCl buffer (pH 9.0) and 50 μL of the suspension was placed in a PS well plate. Liposomes were adhered to the plate surface as described above. As a substrate of GUS, 50 μL of 10 mM Tris-HCl buffer containing 10 μM TokyoGreen-β GlcU (GORYO Chemical, Inc, Sapporo, Japan) was added to each well after washing unbound liposomes. The hydrolysis reaction was detected as the fluorescence signal using the microplate reader at indicated time points. The excitation and emission wavelengths used were 485 and 535 nm, respectively.

Acknowledgements

This work was supported in part by KAKENHI grants 17K14868 (M.I.), 17H00888 (T.M.), 16H00767 (T.M.), and 17H01345 (K.H.) from the Japan Society for the Promotion of Science, and the ImPACT project from the Japan Science and Technology

Agency (T.M.). We thank Kazuho Sawada and Ayane Kawashiri for their technical assistance.

References

1. Good, M.; Trepat, X., Cell parts to complex processes, from the bottom up. *Nature* **2018,** *563* (7730), 188-189.
2. Mizuuchi, R.; Ichihashi, N., Sustainable replication and coevolution of cooperative RNAs in an artificial cell-like system. *Nat. Ecol. Evol.* **2018,** *2* (10), 1654-1660.
3. Mansy, S. S.; Schrum, J. P.; Krishnamurthy, M.; Tobe, S.; Treco, D. A.; Szostak, J. W., Template-directed synthesis of a genetic polymer in a model protocell. *Nature* **2008,** *454* (7200), 122-5.
4. Noireaux, V.; Libchaber, A., A vesicle bioreactor as a step toward an artificial cell assembly. *Proc. Natl. Acad. Sci. USA* **2004,** *101* (51), 17669-74.
5. Urano, Y.; Kamiya, M.; Kanda, K.; Ueno, T.; Hirose, K.; Nagano, T., Evolution of fluorescein as a platform for finely tunable fluorescence probes. *J. Am. Chem. Soc.* **2005,** *127* (13), 4888-4894.
6. Matsubayashi, H.; Kuruma, Y.; Ueda, T., In vitro synthesis of the E. coli Sec translocon from DNA. *Angew. Chem. Int. Ed. Engl.* **2014,** *53* (29), 7535-8.
7. Scott, A.; Noga, M. J.; de Graaf, P.; Westerlaken, I.; Yildirim, E.; Danelon, C., Cell-Free Phospholipid Biosynthesis by Gene-Encoded Enzymes Reconstituted in Liposomes. *PLoS One* **2016,** *11* (10), e0163058.
8. Osawa, M.; Anderson, D. E.; Erickson, H. P., Reconstitution of contractile FtsZ rings in liposomes. *Science* **2008,** *320* (5877), 792-4.
9. Maeda, Y. T.; Nakadai, T.; Shin, J.; Uryu, K.; Noireaux, V.; Libchaber, A., Assembly of MreB filaments on liposome membranes: a synthetic biology approach. *ACS Synth Biol* **2012,** *1* (2), 53-9.
10. Fujii, S.; Matsuura, T.; Sunami, T.; Nishikawa, T.; Kazuta, Y.; Yomo, T., Liposome display for in vitro selection and evolution of membrane proteins. *Nat. Protoc.* **2014,** *9* (7), 1578-91.
11. Fujii, S.; Matsuura, T.; Sunami, T.; Kazuta, Y.; Yomo, T., In vitro evolution of alpha-hemolysin using a liposome display. *Proc. Natl. Acad. Sci. USA* **2013,** *110* (42), 16796-801.
12. Fujiwara, K.; Adachi, T.; Doi, N., Artificial Cell Fermentation as a Platform for Highly Efficient Cascade Conversion. *ACS Synth Biol* **2018,** *7* (2), 363-370.

13. Berhanu, S.; Ueda, T.; Kuruma, Y., Artificial photosynthetic cell producing energy for protein synthesis. *Nat. Commun.* **2019,** *10* (1), 1325.
14. Dwidar, M.; Seike, Y.; Kobori, S.; Whitaker, C.; Matsuura, T.; Yokobayashi, Y., Programmable Artificial Cells Using Histamine-Responsive Synthetic Riboswitch. *J. Am. Chem. Soc.* **2019,** *141* (28), 11103-11114.
15. Lerchner, J.; Wolf, A.; Buchholz, F.; Mertens, F.; Neu, T. R.; Harms, H.; Maskow, T., Miniaturized calorimetry - a new method for real-time biofilm activity analysis. *J. Microbiol. Methods* **2008,** *74* (2-3), 74-81.
16. Donlan, R. M.; Costerton, J. W., Biofilms: Survival Mechanisms of Clinically Relevant Microorganisms. *Clin. Microbiol. Rev.* **2002,** *15* (2), 167-193.
17. Hori, K.; Matsumoto, S., Bacterial adhesion: From mechanism to control. *Biochem. Eng. J.* **2010,** *48* (3), 424-434.
18. Costa, T. R.; Felisberto-Rodrigues, C.; Meir, A.; Prevost, M. S.; Redzej, A.; Trokter, M.; Waksman, G., Secretion systems in Gram-negative bacteria: structural and mechanistic insights. *Nat. Rev. Microbiol* **2015,** *13* (6), 343-59.
19. Wu, T.; Malinverni, J.; Ruiz, N.; Kim, S.; Silhavy, T. J.; Kahne, D., Identification of a multicomponent complex required for outer membrane biogenesis in Escherichia coli. *Cell* **2005,** *121* (2), 235-45.
20. Ohta, N.; Kato, Y.; Watanabe, H.; Mori, H.; Matsuura, T., In vitro membrane protein synthesis inside Sec translocon-reconstituted cell-sized liposomes. *Sci. Rep.* **2016,** *6*, 36466.
21. Linke, D.; Riess, T.; Autenrieth, I. B.; Lupas, A.; Kempf, V. A., Trimeric autotransporter adhesins: variable structure, common function. *Trends Microbiol.* **2006,** *14* (6), 264-70.
22. Ishikawa, M.; Nakatani, H.; Hori, K., AtaA, a new member of the trimeric autotransporter adhesins from *Acinetobacter* sp. Tol 5 mediating high adhesiveness to various abiotic surfaces. *PLoS One* **2012,** *7* (11), e48830.
23. Ishikawa, M.; Shigemori, K.; Hori, K., Application of the adhesive bacterionanofiber AtaA to a novel microbial immobilization method for the production of indigo as a model chemical. *Biotechnol. Bioeng.* **2014,** *111* (1), 16-24.
24. Hori, K.; Ohara, Y.; Ishikawa, M.; Nakatani, H., Effectiveness of direct immobilization of bacterial cells onto material surfaces using the bacterionanofiber protein AtaA. *Appl. Microbiol. Biotechnol.* **2015**.
25. Keppler, A.; Gendreizig, S.; Gronemeyer, T.; Pick, H.; Vogel, H.; Johnsson, K., A general method for the covalent labeling of fusion proteins with small molecules in vivo. *Nat. Biotechnol.* **2003,** *21* (1), 86-9.

26. Gautier, A.; Juillerat, A.; Heinis, C.; Correa, I. R., Jr.; Kindermann, M.; Beaufils, F.; Johnsson, K., An engineered protein tag for multiprotein labeling in living cells. *Chem. Biol.* **2008,** *15* (2), 128-36.
27. Rosano, G. L.; Ceccarelli, E. A., Recombinant protein expression in Escherichia coli: advances and challenges. *Front. Microbiol.* **2014,** *5*, 172.
28. Koiwai, K.; Hartmann, M. D.; Linke, D.; Lupas, A. N.; Hori, K., Structural Basis for Toughness and Flexibility in the C-terminal Passenger Domain of an Acinetobacter Trimeric Autotransporter Adhesin. *J. Biol. Chem.* **2016,** *291* (8), 3705-24.
29. Hernandez Alvarez, B.; Hartmann, M. D.; Albrecht, R.; Lupas, A. N.; Zeth, K.; Linke, D., A new expression system for protein crystallization using trimeric coiled-coil adaptors. *Protein Eng. Des. Sel.* **2008,** *21* (1), 11-8.
30. Uyeda, A.; Watanabe, T.; Hohsaka, T.; Matsuura, T., Different protein localizations on the inner and outer leaflet of cell-sized liposomes using cell-free protein synthesis. *Synth. Biol. (Oxf)* **2018,** *3* (1), ysy007.
31. Yoshimoto, S.; Nakatani, H.; Iwasaki, K.; Hori, K., An Acinetobacter trimeric autotransporter adhesin reaped from cells exhibits its nonspecific stickiness via a highly stable 3D structure. *Sci. Rep.* **2016,** *6*, 28020.
32. Ishikawa, M.; Yoshimoto, S.; Hayashi, A.; Kanie, J.; Hori, K., Discovery of a novel periplasmic protein that forms a complex with a trimeric autotransporter adhesin and peptidoglycan. *Mol Microbiol* **2016,** *101* (3), 394-410.
33. Yoshimoto, S.; Ohara, Y.; Nakatani, H.; Hori, K., Reversible bacterial immobilization based on the salt-dependent adhesion of the bacterionanofiber protein AtaA. *Microb. Cell. Fact.* **2017,** *16* (1), 123.
34. Frohnmayer, J. P.; Bruggemann, D.; Eberhard, C.; Neubauer, S.; Mollenhauer, C.; Boehm, H.; Kessler, H.; Geiger, B.; Spatz, J. P., Minimal synthetic cells to study integrin-mediated adhesion. *Angew. Chem. Int. Ed. Engl.* **2015,** *54* (42), 12472-8.
35. Nishiya, T.; Kainoh, M.; Murata, M.; Handa, M.; Ikeda, Y., Reconstitution of adhesive properties of human platelets in liposomes carrying both recombinant glycoproteins Ia/IIa and Ibalpha under flow conditions: specific synergy of receptor-ligand interactions. *Blood* **2002,** *100* (1), 136-142.
36. Bartelt, S. M.; Chervyachkova, E.; Ricken, J.; Wegner, S. V., Mimicking Adhesion in Minimal Synthetic Cells. *Adv. Biosyst.* **2019,** *3* (6), 1800333.
37. Kurokawa, C.; Fujiwara, K.; Morita, M.; Kawamata, I.; Kawagishi, Y.; Sakai, A.; Murayama, Y.; Nomura, S. M.; Murata, S.; Takinoue, M.; Yanagisawa, M., DNA cytoskeleton for stabilizing artificial cells. *Proc. Natl. Acad. Sci. USA* **2017,** *114*

592 (28), 7228-7233.

593